Acta Botanica Brasilica - 34(4): 633-644. October-December 2020.
doi: 10.1590/0102-33062020abb0140

Early development of epiphytic roots: perspectives based on the composition of the velamen cell wall

Luísa Gouveia Lana[1], Ana Flávia de Melo Silva[1], Aldineia Buss[1], Denis Coelho de Oliveira[1] and Ana Silvia Franco Pinheiro Moreira[1*]

Received: April 8, 2020
Accepted: July 20, 2020

ABSTRACT

The velamen, a root structure of some epiphytic species for water uptake, usually is stratified epidermis consisting of dead cells. In general, its cell walls exhibit variation during development, including in thickness and amount and type of impregnated substances. These changes result in diverse physical and chemical properties that can serve in water and nutrient uptake, as well as in mechanical support and protection. On this basis, the main objective of the current study was to describe the composition of the cell walls of the velamen during the development of the roots of four species of *Cattleya*. Anatomical, histochemical and immunocytochemical analyses were performed with samples (n=3 individuals per species) of meristematic, developing, and mature regions of the root. The development of the primary wall led to the deposition of pectins as highly methylesterified homogalacturonans, which were demetihylesterified with maturation of the velamen. The deposition of lipids (and subsequently lignins) in velamen cells marked a transition stage to the formation of the secondary wall, which gives rigidity to the tissue. For the first time, we showed that the deposition of lipids and lignins began close to the exodermis in the direction of the epivelamen.

Keywords: *Cattleya*, Orchidaceae, pectins, root meristem, velamen development

Introduction

The morphological and anatomical features of the roots of epiphytic orchids have evolved in order to improve water and nutrient uptake, since these plants grow under severe fluctuations of these resources (Krauss 1948; Proença & Sajo 2008; Macedo 2013). One of these remarkable features is the velamen, considered to be an adaptive trait responsible for the efficient absorption of water and nutrients (Engard 1944; Silva & Milaneze-Gutierre 2004; Zotz & Winkler 2013). The velamen is the most external root tissue of many epiphytic groups and of other related terrestrial plants, mainly monocots (Zotz & Winkler 2013). Usually, the velamen consists of a stratified epidermis resulting from periclinal divisions of the protodermis, dead at maturity, and composed of compactly arranged cells with different secondary thickenings in the cell walls (Engard 1944; Pridgeon 1987; Joca *et al*. 2020). The composition of cell walls during plant organ development, including secondary thickenings, seems to be impacted by abiotic factors that change the physical, chemical and physiological properties of the cell walls (Albersheim *et al*. 2010; Le Gall *et al*. 2015).

1 Instituto de Biologia, Universidade Federal de Uberlândia, 38400-902, Uberlândia, MG, Brazil

* Corresponding author: anasilviamoreira@gmail.com

The dynamic and complex arrangement of the cell wall components, associated with diverse physicochemical properties, triggers many signaling events that are responsible for cellular functions, such as patterns of organ and tissue development and growth (Lorenzo *et al*. 2019). This differential arrangement occurs early during cell wall development (Burton *et al*. 2010), leading to primary and/or secondary wall formation (Kraus *et al*. 2012; Canteri *et al*. 2019; Kang *et al*. 2019). The primary cell walls (PCW) are formed during cell division and early expansion, and are mainly composed of cellulose, hemicelluloses and pectins. The cellulose microfibrils are embedded in a hydrated matrix of polysaccharides which forms a three-dimensional network responsible for the physical, chemical and physiological properties of cell walls (Cosgrove 2005; Amar *et al*. 2010; Albersheim *et al*. 2010). The formation of the secondary cell wall occurs by lignin deposition, especially after cell expansion (Albersheim *et al*. 1996; Cosgrove & Jarvis 2012; Fahey *et al*. 2017). Although formed by dead cells at maturity, with expressive secondary thickenings, the cell walls of the velamen retain a pectic matrix. These pectins with different degrees of methylesterification seem to be essential for stability, mechanical support of the velamen cells, and even the dynamics of nutrient absorption (Joca *et al*. 2020). The main domains of pectins are the homogalacturonans (HGs) (Ridley *et al*. 2001; Willats *et al*. 2001), which play an important role in gel formation that in turn increases water retention and, with the presence of Ca^{2+}, may lead to cell wall stiffening (Liu *et al*. 2013; Albersheim *et al*. 2010). They are also related to water absorption by apoplastic flow and may be involved in mechanical protection and reduction of water loss (Albersheim *et al*. 1996; Willats *et al*. 2000). The role of each component of the cell wall in the roots of orchids and the degree of pectin methylesterification may be involved in the capacity of water absorption, retention and transport (Willats *et al*. 2001; Joca *et al*. 2017, 2020). In addition, the pectic matrix can act as a moderator of cationic exchanges since naturally negatively charged carboxyl groups (COO-) can attract positively charged compounds (Zotz & Winkler 2013; Joca *et al*. 2020).

The deposition of suberin and lignins occurs in the final stages of development of the primary wall and during the formation of the secondary wall of velamen cells. Both are first placed mainly in the middle lamella of the cell, related to adaptations and specialized physiological functions of tissue (Monties 1989; Campbell & Sederoff 1996; Zeier & Schreiber 1997). Lignins provide mechanical stability, whereas suberin, a highly hydrophobic substance, impermeabilizes the cell walls, thus increasing the apoplastic flow in the velamen and obstructing this flow in the exodermis and endodermis (North & Nobel 1994; Enstone & Peterson 2005; Franke & Schreiber 2007; Joca *et al*. 2017). The compactation and chemical composition (including suberin and often the addition of lignin) of the basic cells of the exodermis and endodermis force the passage of water and nutrients through the passage cells as a preselection of solutes before reaching the vascular cylinder (Zimmermann *et al*. 2000; Hose *et al*. 2001; Franke & Schreiber 2007). Lignins also play a role in apoplastic flow throught the cortex (sometimes as a barrier or as structures leading towards the stele) (Joca *et al*. 2017) and, together with lignified cells of the exodermis, provide mechanical protection and decrease the loss of water from the cortex into the environment (Sanford & Adanlawo 1973; Benzing *et al*. 1982; Ma & Peterson 2003).

The adventitious roots in orchids have root apical meristems (RAM) with their epidermis associated with cortex and not with rootcap production (Heimsch *et al*. 2008). In orchids, RAM are closed, with cortical-epidermal initial cells or cortical initials separated from the epidermal initials. In addition, RAM show a bulge of the outer cortical initials towards the lateral rootcap (Heimsch *et al*. 2008). The early development of the roots from the RAM is decisive in order to determine the functions assigned to the roots. The periclinal divisions will determine the number of cell layers of the velamen (Engard 1944), while cellular development will end with the formation of a secondary cell wall which maximizes water and nutrient uptake (Zotz & Winkler 2013; Joca *et al*. 2017; 2020). Thus, we believe that the time of velamen differentiation may be related to the composition of the cell walls (including suberin impregnation and/or secondary wall development). In the present study, we describe the composition of the velamen cell wall during early development and up to root maturation of four species of *Cattleya* in an attempt to understand the patterns of pectin, lipid and lignin deposition. *Cattleya* is a native genus from Brazil, composed by epiphytic species, and with a velamen usually described with many cell layers.

Materials and methods

Plant material

In the current study we used four species of *Cattleya*: *C. nobilior* Rchb.f., *C. schilleriana* Rchb.f., *C. velutina* Rchb.f. and *C. walkeriana* Gardner, kept in the greenhouse of Universidade Federal de Uberlândia, Uberlândia, Brazil. The greenhouse was maintained in natural conditions. The temperature ranged from 12 °C to 33 °C (annual average of 22 °C), and the maximum photosynthetic active radiation was 250 μmol m^{-2} s^{-1}. The plants received free water supply until percolation in the pots. Fragments of the root apices and mature roots (3 cm from the apex) were collected and fixed in 70% FAA (formaldehyde: acetic acid: 70% ethanol, 1:1:18, v:v:v) for 48 hours, and subsequently stored in 70% ethanol (Kraus & Arduin 1997).

Histological analyses

Samples of *Cattleya* roots (three individuals per species) were free-hand sectioned at 3 cm from the apex to confirm

the mature condition of the velamen. The sections were cleared with 50 % sodium hypochlorite (Kraus & Arduin 1997) and stained with 1 % safranin alcoholic solution and 0.5 % Astra blue (1:9 v/v) (Bukatsch 1972). Samples were glued on slides, assembled with glycerinated gelatin of Kaiser (Johansen 1940) and the material was photographed with a Leica® DM500 photomicroscope coupled to a Leica® ICC50 HD digital camera. The transverse area of the roots, the number of cell layers and the thickness of the velamen, as well as the area of the root occupied by the velamen were determined in ten roots with free growth (not adhered to a substrate) per species selected from the three individuals of each species. The Image J software was used (National Institute of Health, EUA) to measure three different points of each section and the mean value was calculated and used as a valid value. Data showed normal distribution and were analysed using ANOVA with posterior Tukey test to compare root area and velamen thickness thickness/area. We assumed differences below 5 % of probability.

RAM structure was analyzed on 4 cm long fragments from the apices, which were divided into three morphological regions; (a) meristematic region (purplish/brown region of the root closest to the RAM), (b) developing region (green, but with many white patches) and (c) mature region (completely white) (Fig. 1A). All samples were dehydrated in ethanol series, pre-infiltrated with 95 % ethanol and base resin 1:1 (v/v) for approximately 36 hours and embedded in base resin according to Historesin® manufacturer instructions (Leica® Biosystem). Sections (~5 µm thick) were cut with a microtome (YD315, ANCAP, Brazil) using disposable high quality stainless-steel razors, stained with 0.05 % toluidine blue in 100 ml of 0.1 M phosphate buffer, pH 4.0 (O'Brien *et al*. 1965) and analyzed with a Leica® DM500 photomicroscope coupled to a Leica® ICC50 HD digital camera.

For scanning electron microscopy (SEM) analyses, root fragments of the orchid species (0.5 cm – meristematic region; and 3 cm from the apex – mature region) were fixed in Karnovsky (4 % paraformaldehyde, 0.01 M glutaraldehyde and 0.2 M phosphate buffer, pH 7.2) (5:3:2, v:v:v) (Karnovsky 1965, modified by Kraus & Ardiun 1997) for at least 48 h, washed and stored in 70 % ethanol and phosphate buffer. The samples were immersed in osmium tetroxide for 1 minute, dehydrated in ethyl series and submitted to CO_2 critical point (EMCPD 300, Leica, Vienna, Austria). The fragments were metallized with gold (20 to 30 nm thick) using a Sputter Coater SCD O50, BalTec (Quorum, New York) and analyzed by SEM (VEGA 3, TESCAN, Czech Republic) calibrated at an acceleration of 10 kV voltages (as used by Pridgeon *et al*. 1983; Porembski & Barthlott 1988).

Histochemical analyses

For lipid detection in the velamen, samples were incubated in a 0.5 % ethanolic solution (80 % ethanol) of Sudan III for 20 to 30 minutes (Sass 1951). For histolocalization of lignins, the sections were incubated with a 1 % phloroglucinol ehtanolic solution (95 % ethanol) and 25 % hydrochloric acid solution for five minutes (Johansen 1940). We also used a DAPI filter (excitation spectrum: 385-400 nm) in an epifluorescence system (Chomicki *et al*. 2014; Joca *et al*. 2017) of a Leica® DM4000B microscope coupled to a Leica® DFC3000 G camera. For all analyses, blank sections were examined in order to confirm false-positive results, as recommended by the cited authors. All sections were mounted in distilled water and photographed using a Leica® DM500 microscope coupled to a Leica® ICC50 HD digital camera.

Immunocytochemical analyses

Samples of the apices and mature roots were embedded in Leica® historesin, sectioned (10 µm) with a rotatory microtome (YD315, ANCAP, Brazil) and incubated in block solution (3 % powdered milk protein, Molico®, in phosphate buffered saline (PBS), pH 7.1) for 30 minutes to prevent crosslinking. Samples were then incubated with the following primary monoclonal antibodies: JIM 5 - for HG epitopes with up to 40 % methylesterification and JIM7 - for HGs epitopes with up to 80 % methylesterification (Centre for Plant Sciences, University of Leeds, UK), for one hour. Next, the samples were washed in PBS and incubated with IgG anti-rat FITC secundary antibody (Sigma-Aldrich®) (1:100 in 3 % milk protein/PBS) for two hours in the dark. As a control, the primary antibody was suppressed. After a new washing in PBS, the sections were mounted in glycerin/distilled water (1:1) and examined under a Leica® DM500 microscope with an epifluorescence system coupled to a Leica® ICC50 HD digital camera, using an FITC filter (Blake *et al*. 2006; Hervé *et al*. 2011; Leroux *et al*. 2018 – modified).

Results

In the apices of the four *Cattleya* roots, the velamen contained living cells close to the RAM, but development began very early to lead to maturity, when some dead cells could be noted. The complexity of the velamen's cell wall increased with maturity, including the deposition of lipids and lignins. During primary development, we observed the presence of high-methyesterified pectins predominantly in younger tissues. These pectins were also detected in the mature velamen of *C. velutina* and *C. walqueriana*. Low methylesterified HGs predominated in mature velamen of *C. velutina*, *C. walqueriana* and *C. nobilior*.

Structural analysis of ***Cattleya*** *roots*

The roots of *Cattleya nobilior* had the smallest transverse sectional area (5.21 ± 1.6 mm²), while *C. velutina* had the most calibrous roots (11.80 ± 2.4 mm²), and *C. schilleriana* and *C. walquerian* had similar areas (~ 7.8 ± 1.9 mm²)

(Tab. 1). The roots were cylindrical in shape, while the roots in contact with a substrate were slightly flattened. The meristematic and developing regions (characterized by still green or sometimes brownish coloration) at the root apex were about 11.4 ± 0.14 mm long in all species, becoming white at maturity (Fig. 1A). A slight purplish/brown coloration was observed (up to 1.0 cm of the RAM) in all species due to anthocyanins in the vacuoles of the ground meristem and/or cortical parenchyma cells (Fig. 1B-C).

The four species showed the typical root structure of other epiphytic orchids, composed of a vascular cylinder, cortical parenchyma limited by endodermis and exodermis, and a multilayered velamen (Fig. 2). The vascular cylinder had 13 to 17 strands of xylem and phloem in *C. nobilior*, 12 to 18 in *C. schilleriana* (Fig. 2A), 16 to 20 in *C. velutina* and 13 to 18 in *C. walqueriana*. In all species, the vascular cylinder was limited by an O-thickened endodermis (Fig. 2B) impregnated with lipids (Fig. 2C) and lignins (Fig. 2D), except in passage cells. The cortical parenchyma had cells with different types of cell wall thickenings, such as uniform thickenings - always impregnated with lipids and/or lignins (Fig. 2C-E), or phi-thickenings in *C. schilleriana*, *C. walqueriana* and *C. velutina* (Fig. 2F). The exodermis externally limits the cortical parenchyma and, just like the endodermis, had cell walls impregnated with lipids and/or lignins (Fig. 2G-J).

The velamen occupied about 33 % of the total root area in *C. schilleriana* and *C. velutina*, and almost 50 % of it in *C. nobilior* and *C. walkeriana* (Tab. 1).The number of velamen cell layers varied with the position around the circumference of the root; the regions flattening with the substrate had fewer numbers of layers, while the free growing areas showed a higher number of layers. Four to eight cell layers were observed in *C. nobilior*, two to six in *C. schilleriana*, four to nine in *C. velutina*, and four to seven in *C. walqueriana*.

The RAM comprised the "closed" type with a slight bulge of the outer cortical initials towards the lateral rootcap, curving along the base of the columella (Fig. 3A, B, C). The cells of the protodermis divided periclinally still under the root cap, with many layers under its lateral margins (Fig. 3B). Lignins and lipids were not detected in the velamen cells close to the RAM, but were gradativelly deposited in the velamen cell walls, lipids first and mainly around the exodermis, and lignins later in all cell walls of the velamen. The mature cell walls of all studied species had similar thickening patterns, with many pores (Fig. 3D, E, F). Still in the green region of the apex (developing region), about 1 cm from the RAM, it was possible to observe many dead cells in the velamen forming white patches (Fig. 1A). At approximately 12 mm from the RAM, the velamen was fully mature in all species, with all cells dead, completely filled with air and of white color.

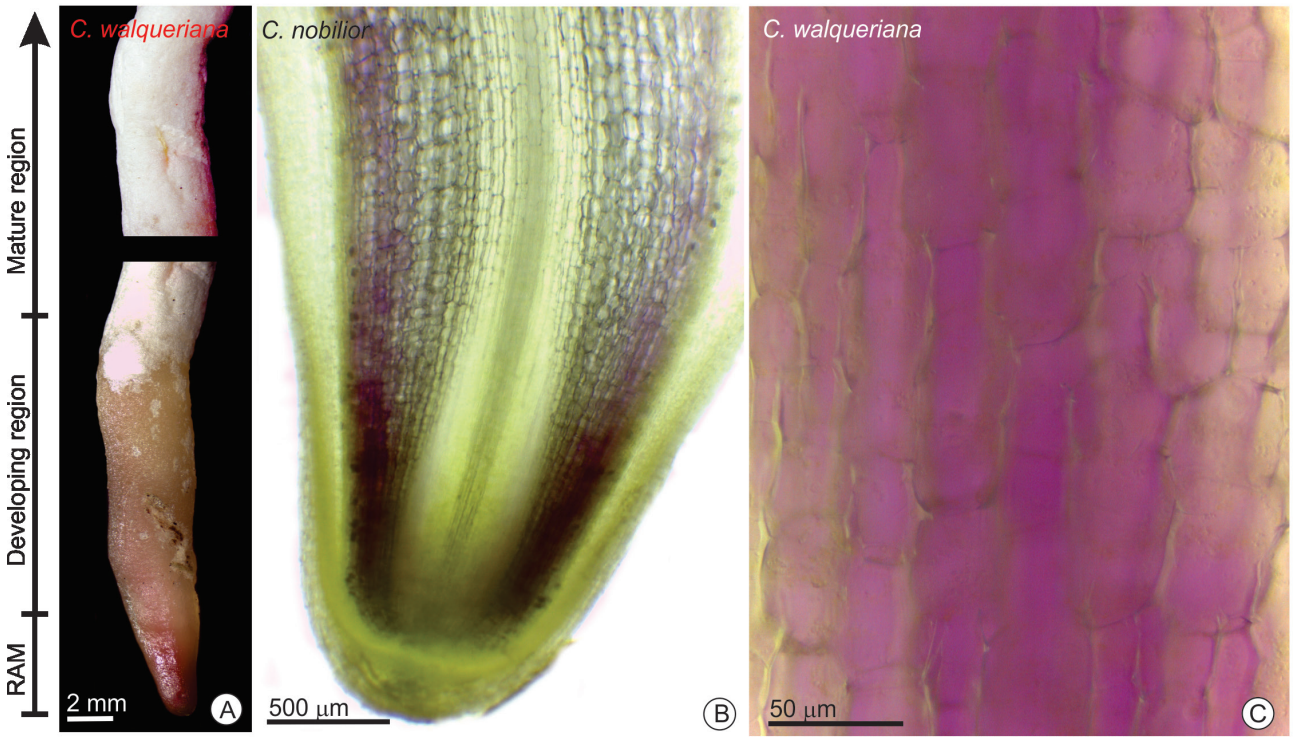

Figure 1. Root apex of three distinct species of *Cattleya*. The roots were divided into three morphological regions: (1) meristematic region (RAM), (2) developing region and (3) mature region. **A.** The three morphological regions of *C. walqueriana* root. **B.** Longitudinal section of *C. nobilior* root showing the presence of anthocyanins in the meristematic region (ground meristem). **C.** A detail of the cells of the ground meristem in *C. walqueriana* roots with anthocyanin-filled vacuoles.

Table 1. Root area and the investment in velamen by *Cattleya nobilior*, *C. schilleriana*, *C. velutina* and *C walqueriana*. All species were kept in a greenhouse for approximately one year.

	Root area (mm^2) in transverse section	Area of velamen in transverse section (mm^2)	Velamen thickness (µm)
Cattleya nobilior	5.21 ± 1.6^c	2.47 ± 1.0^b	380.2 ± 83.8^a
Cattleya schilleriana	7.87 ± 2.0a^b	2.64 ± 0.9^b	333.5 ± 93.3^a
Cattleya velutina	11.80 ± 2.4^a	4.00 ± 1.0^a	407.2 ± 93.2^a
Cattleya walkeriana	7.88 ± 1.7^b	3.41 ± 0.9^{ab}	436.9 ± 81.1^a
P	<0.0001	<0.005	>0.05

The data compared species using ANOVA with posterior Tukey test considering differences below 5 %.

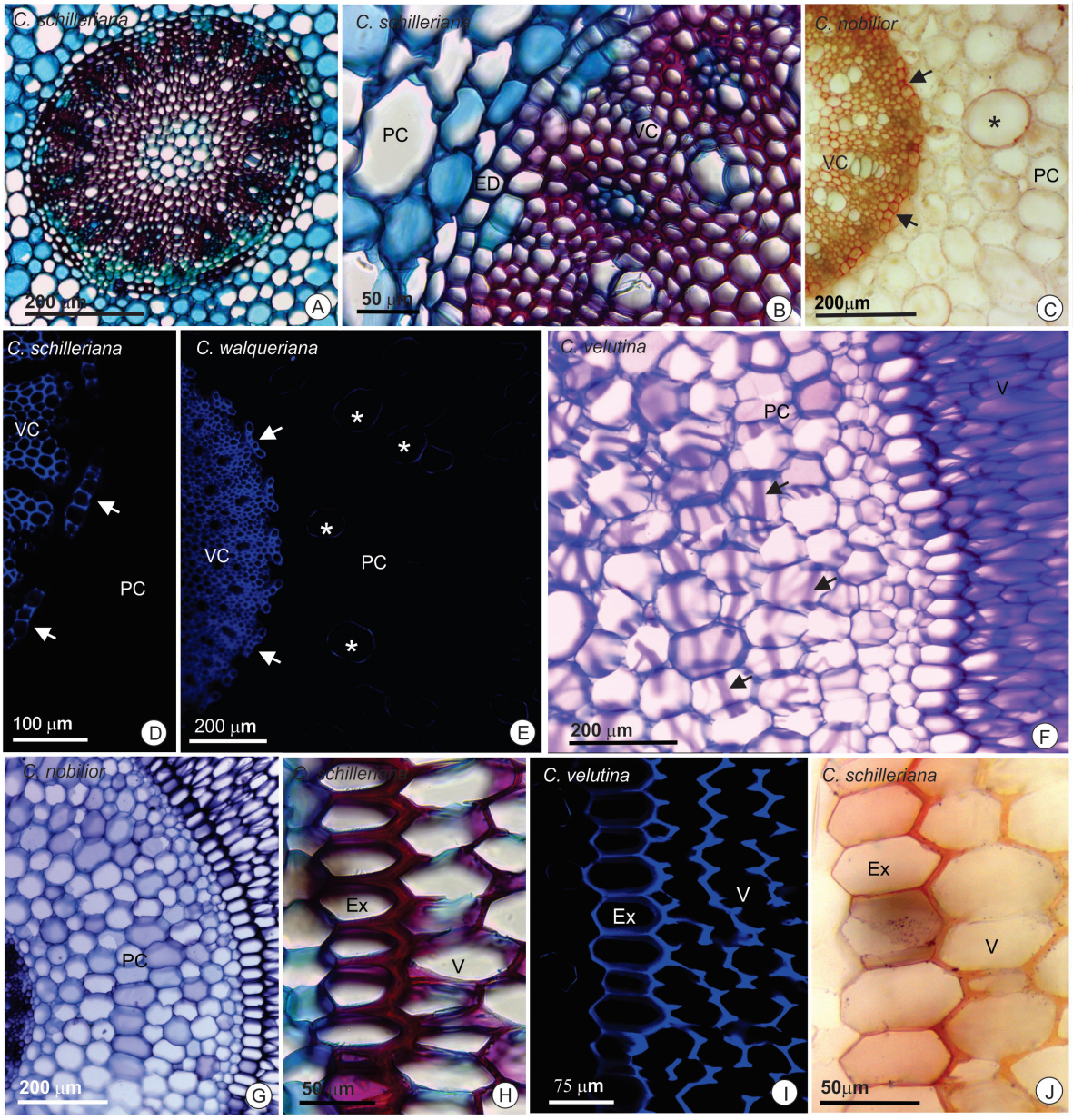

Figure 2. Root anatomy of four different species of *Cattleya*. **A.** Overview of a vascular cylinder in *C. schilleriana* showing 13 xylem and phloem strands. **B.** Detail of a vascular cylinder, with xylem and phloem strands and O-thickened endodermis. **C.** Cross sections stained with Sudan III (red color) in *C. nobilior* roots. O-thickenings in the endodermis (arrows) and isolated cells in the cortical parenchyma with uniform thickenings (*) impregnated with lipids. **D-E.** Lignins detected with a fluorescent microscope using a DAPI filter. **D.** O-thickenings (arrows) in the endodermis, and **E.** uniform thickenings (*) in the parenchymatic cortex. **F.** Parenchymatic cortex with phi-thickenings (arrows). **G.** Overview of a *C. nobilior* root. **H.** Detail of the exoderm with U-thickenings in *C. schilleriana*. **I.** U-thickened exodermis and velamen cells impregnated with lignin (image using DAPI filter) in *C. velutina*. **J.** U-thickened exodermis impregnated with lipids in *C. schilleriana*. (ED – endodermis, Ex – exodermis, PC – parenchymatic cortex, V – velamen, VC – vascular cylinder).

Inmunocytochemical analysis: distribution and degree of methylesterification of pectins in the velamen

The epitopes of HGs did not label the RAM in any of the species of *Cattleya*, but labeled the young and mature tissue. Except for *C. nobilior*, HG epitopes with a high degree of methylesterification recognized by JIM7 labeled the velamen cells in young regions. In mature roots of *C. nobilior*, these HGs with a high degree of methylesterification weakly labeled the cell junctions of the velamen (Fig. 4A), but strongly labeled the region around all cell walls of *C. velutina* (Fig. 4B) and *C. walqueriana*. No epitopes were recognized

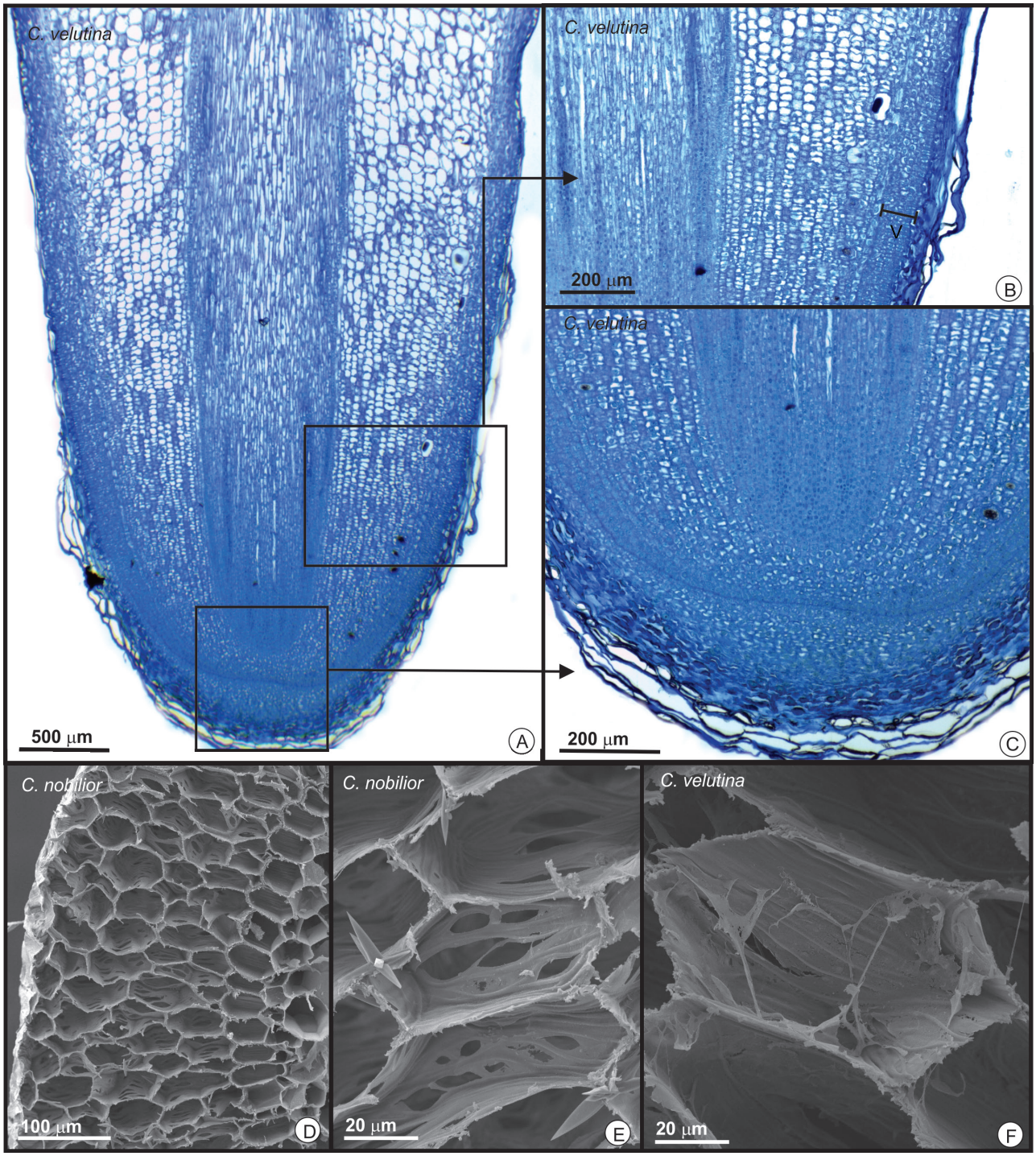

Figure 3. Root apical meristem (RAM) (in longitudinal sections) and mature velamen (transverse sections using scanning electron microscopy) in *Cattleya*. **A.** Overview of the apex of the *C. velutina* root. **B.** Detail of the young velamen still protected by the root cap. **C.** Detail of the RAM of the closed type. **D.** Mature velamen with dead cells in *C. nobilior*. **E.** Detail of the velamen cells with wall thickenings and many pores in *C. nobilior*. **F.** Detail of the velamen cells with wall thickenings in *C. velutina*.

by JIM7 in the velamen cells of *Cattleya schilleriana*. About 1 cm from the apex, when the velamen cells began to die, the epitopes of HGs with up to 40% methylesterification begins to appear, weakly recognized by JIM5, in the cellular junctions of *C. nobilior* (Fig. 4C). In completely mature roots, these epitopes recognized by JIM5 strongly labeled the velamen cells of *C. walqueriana, C. velutina* (Fig. 4D) and *C. nobilior*. In *C. schilleriana*, we only observed lower intensity of labeling in velamen cells (Fig. 4E).

The presence of lipids in the velamen cell walls

Histochemical assays showed deposition of lipids in the cell walls during the development of the velamen (Fig. 5). Deposition gradually begins near the exodermis (Fig. 5A), increasing throughout the velamen with maturation, except in the epivelamen (Fig. 5B). In *C. velutina*, red color for lipids was observed in all cell walls of the velamen, even with maturation (Fig. 5B-C). However, in the other three species, the construction of the secondary cell wall seemed to hide this coloration. In this case, the lipds were conserved in the lamella media (mainly in contact with the exodermis – Fig. 5D-F). In *C. schilleriana*, lipid deposition occured later than in the other orchid analyzed.

Secondary wall development - deposition of lignins in velamen cells

Using fluorescence microscope with a DAPI filter (Fig. 6), we observed that velamen lignification began near the exodermis (centrifuge), where maturation occurred first (as observed in *C. schilleriana* - Fig. 6A-D). The deposition of lignins in the velamen was gradual throughout the root apex and restricted to the secondary cell walls (Fig. 6E-

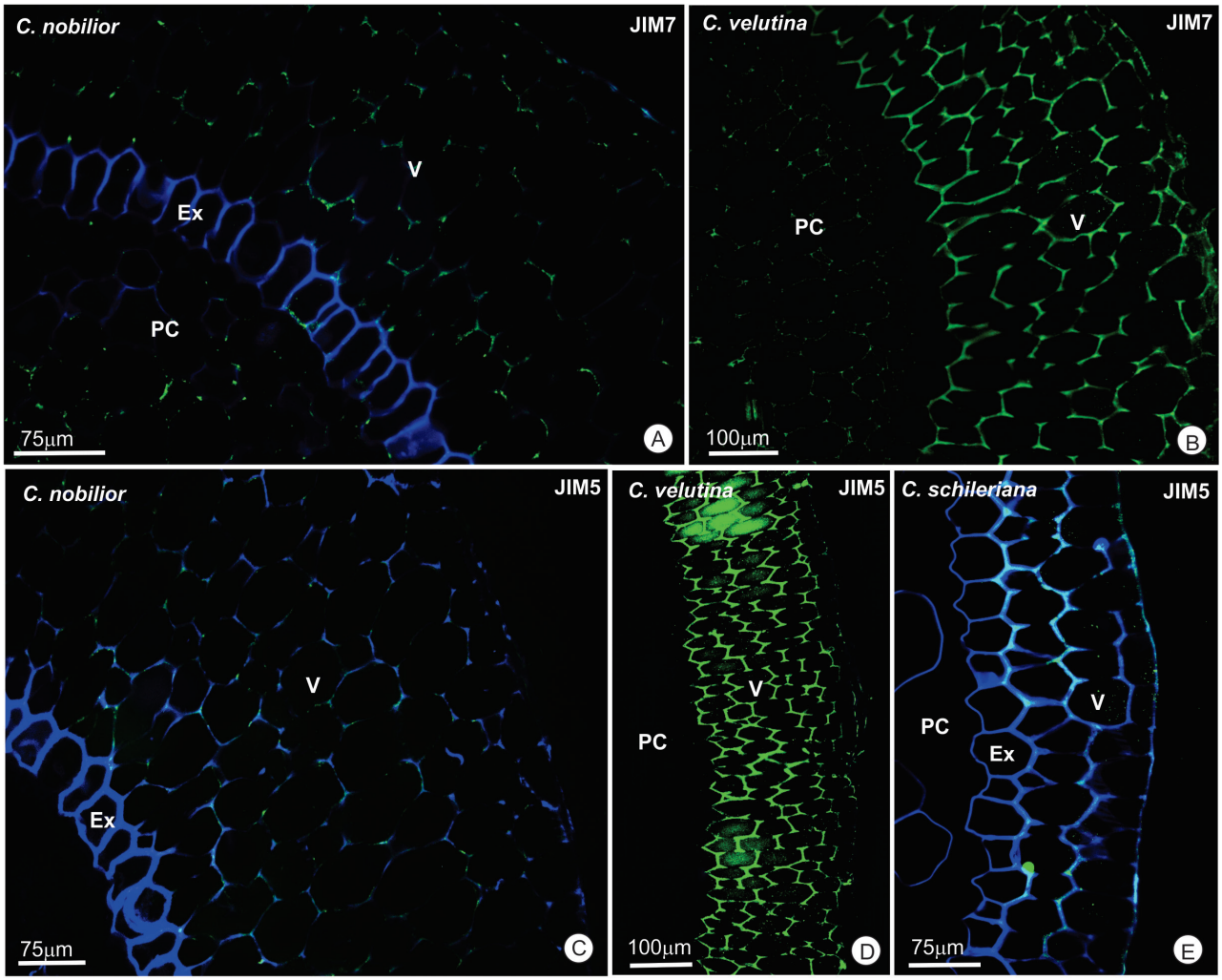

Figure 4. Homogalacturonans of high and low methylesterification labeled by JIM7 and JIM5 antibodies, respectively, in roots of *Cattleya*. The positive reactions are represented by the green color in all images. The blue color (A, C and E) comes from an overlap processing using DAPI filter and shows lignin. **A.** Positive result for JIM7 at the cellular junctions of the velamen in *C. nobilior* in the developing region of the roots. **B.** Positive result for JIM7 in the mature region of the velamen in *C. velutina* roots. **C.** Very weak result for JIM5 in the developing region of *C. nobilior* roots. **D.** Positive result for JIM5 in the mature region of the velamen in *C. velutina*. **E.** Weak result for JIM5 in the mature region of the velamen in *C. schilleriana*. (Ex – exodermis, PC – parenchymatic cortex, V – velamen).

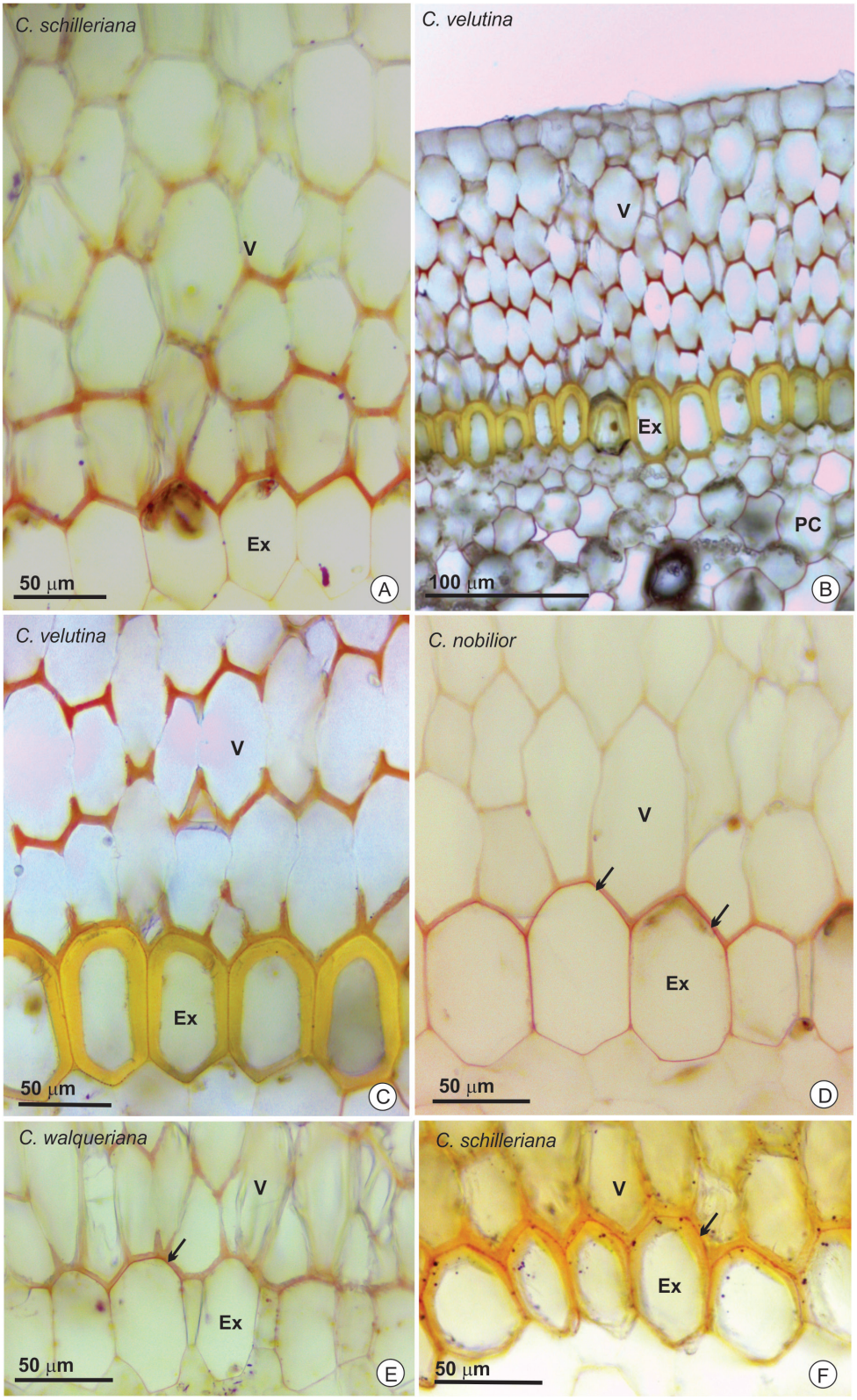

Figure 5. Histochemical test with Sudan III for the detection of lipids in *Cattleya* roots. A positive reaction is indicated by the red color. **A.** Velamen with centrifugal deposition of lipids in the developing region of the *C. schilleriana* roots. **B-C.** Lipids in mature roots of *C. velutina*. **(B)** An overview of the velamen and exodermis and **(C)** a detail showing the velamen cell walls and the media lamella of the exodermis. **D.** Detail of the velamen cells with a positive result in the developing region of the roots of *C. nobilior*. **E.** Positive results in the velamen cell of the mature region of *C. walqueriana*. **F.** Positive results in the velamen cell of the mature region of *C. schilleriana*. (Ex – exodermis, PC – parenchymatic cortex, V – velamen).

I). We could not detect lignin deposition in regions near RAM (Fig. 6I) and we first detected it in cellular junctions of *C. velutina* (Fig. 6G-H) and *C. nobilior*. Despite the later deposition of lipids in *C. schilleriana* when compared to the other species, in this species, lignins were detected early in a younger velamen, prominently in the developing region. In mature roots with complete cell wall development, lignins were detected throughout the velamen as well as in cells of the epivelamen in all studied species.

Discussion

All species of *Cattleya* roots studied here had similar tissue composition, as described for other species of epiphytic orchids (Krauss 1948; Moreira & Isaias 2008; Moreira *et al*. 2013; Joca *et al*. 2017). In all roots, the division of the protodermal cells in the RAM was of the closed type (according to Heimsch *et al*. (2008) classification). We detected pectins, lipids and lignins during the development of the velamen cell wall. HGs with a high methylesterification degree labeled the velamen cells in young regions, mainly in *C. velutina* and *C. walqueriana*. About one centimeter from the apex, when the velamen cells began to die, the epitopes of HGs with up to 40 % methylesterification began to appear, strongly labeled in mature roots of *C. walqueriana, C. velutina* and *C. schilleriana*. Cell wall complexity increased during root differentiation, with lipids appearing first, followed by lignins. The deposition of these substances was centrifugal, initiating near the exodermis in the direction to the epivelamen.

Development of the velamen in ***Cattleya*** roots

The velamen is a tissue that undergoes programmed cell death (Pridgeon 1987), being mature when all its cells are dead. In the four species studied, the formation of the velamen began with the division of the protodermal cells still under the root cap at the apex of the root. This is not a pattern for all orchid species, as shown in *Anathallis sclerophylla* in which the cell divisions for velamen formation occurs only after the disappearance of the root cap (Kedrovski & Sajo 2019). As observed for other species of orchids (Heimsch *et al*. 2008), the apical meristems had a closed-type architecture, with the initials of the root cap, cortex and vascular cylinder separated. The epidermal initials were associated with the cortex and not attached to the root cap initials.

Cattleya velutina had more calibrous roots than the other species studied, but *C. nobilior* and *C. walkeriana* were the species that showed more investment in this tissue (area occupied by the velamen). The only species that seemed to show different timing in maturation of the velamen cells was *C. schileriana*. This species did not show a wider velamen diameter, indicating that there is no relation between these traits and the timing of maturation of velamen cells. Some strategies such as a larger number of xylem strands aligned with the endodermal passage cells, cortical thickenings and the investment in velamen can maximize the apoplastic flow in the direction to the xylem (Joca *et al*. 2017). Thus, the rapid maturation of the velamen (including lipid and lignin deposition) can be interesting in order to maximize water uptake. In addition, root caliber is not indicative of investment in the velamen, but it is known that the greater investment in this tissue, the higher water and nutrient uptake (Joca *et al*. 2017). Thin roots such as those of *C. nobilior* and *C. walkeriana* had about 50 % of their area occupied by the velamen, demonstrating the importance of this tissue for resource absorption.

Analysis of the velamen cell wall composition

During the development of the velamen, chemical and structural changes in the cell walls occur until this structure reaches stability in the mature root. In this study, we detected a spatial-temporal variation in the deposition of cell wall components during the development of the velamen in four species of *Cattleya*. The differential distribution of pectins, lipids and lignins, in a general way, guarantees the mechanical resistance of plant tissues, being also involved in apoplastic and symplastic water flow (Albersheim *et al*. 1996; Albersheim *et al*. 2010; Joca *et al*. 2017). In addition, hydrophobic compounds in the velamen may be related to water retention inside the organ (Kedrovski & Sajo 2019) and to protection against photooxidation (Chomicki *et al*. 2015).

The plant cell wall formation is based on nanocomposites of cellulose microfibrils incorporated into different matrix polymers (Gierlinger *et al*. 2013; Fahey *et al*. 2017; Kang *et al*. 2019). The celluloses are rigid and are embedded in a matrix rich in water, hemicellulose, pectins and proteins, that together constitute the primary cell wall (Pridgeon 1987; Macedo 2013). Cellulose is a polysaccharide composed of (1 → 4) -β-D-glucopyranose units (Newman 2004) and is considered to be a crystalline polymer. This crystalline polymer is associated with pectins, and ogether increasing cell porosity, adhesion and flexibility (Jarvis 1984; Albersheim *et al*. 2010). One of the most abundant kinds of pectins, the HGs, has been associated with cellular development, cell wall porosity and adhesion, as well as rigidity (Wolf *et al*. 2009). HGs are produced in the Golgi complex in a highly methylesterified condition (exhibiting up to 80 % methyl esterification) (Ralet *et al*. 2008, Wolf *et al*. 2009). In the current study, HGs were not detected in the RAM of the four species of *Cattleya*. However, HGs were detected in highly methylesterified forms as the cells of velamen reached maturation. During the process of maturation, the HGs are de-methylesterified, and the low methylesterified forms of HGs then become predominant in the mature tissue. The presence of HGs with low and high methylesterification in the velamen cells could maintain tissue stability and the necessary flexibility during the

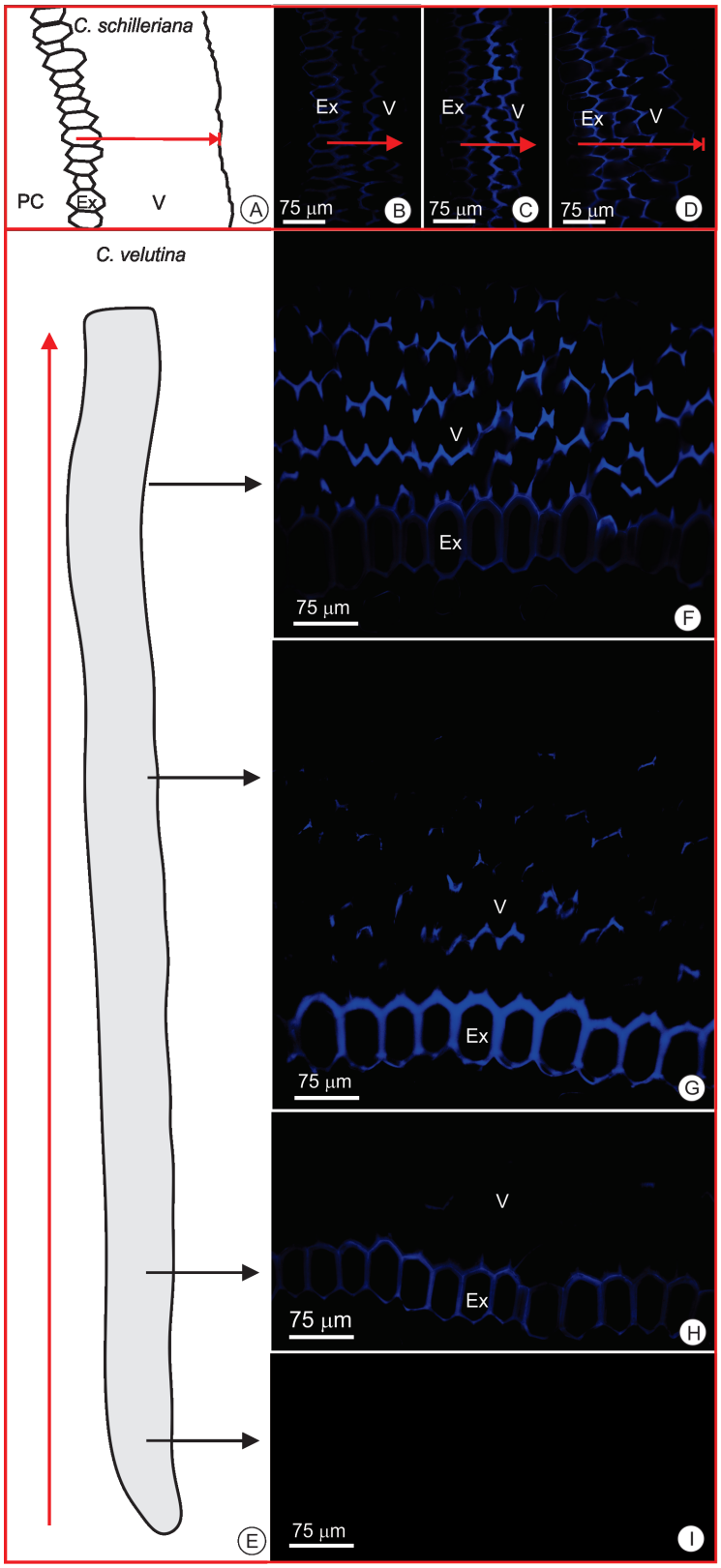

Figure 6. Lignin fluorescence using a DAPI filter in cross sections of *Catlleya* roots. **A-D.** Centrifugal deposition of lignins in the velamen cells of *C. schilleriana*. The red arrows represent the direction of lignin deposition and tissue maturation. **A.** Schematic drawing representing the mature roots. **B**-**C.** Developing region. **D.** Mature velamen. **E-I.** Detection of lignins at different times of maturation in *C. velutina* roots. **E.** Schematic drawing representing the root apex and the direction of tissue maturation (red arrow). **F.** Mature velamen. **G-H.** Developing regions. **I.** Root apex meristem (RAM). (Ex – exodermis, PC – parenchymatic cortex, V – velamen).

processes of development and next water and nutrient uptake. However, as observed in many other orchid species the pettern of HG distribution was not the same for all species (Joca *et al*. 2020).

Non-methylesterified pectins can lead to Ca^{2+} binding and the formation of gels which impart greater stiffness to the wall (Wolf *et al*. 2009). In addition to biophysical changes in the cell wall, changes in the degree of methyl-esterification may lead to the formation of pectic oligogalacturonide (small products of HG breakdown). These molecules act as analog hormone signals that neutralize the action of auxins, regulating cellular development (Ridley *et al*. 2001). In this context, the regulation of enzymatic activity in the degree of methylesterification of HGs may play some role in the control of cell growth (Wolf *et al.* 2009). In the velamen, in regions where the cells begin to die (about one centimeter from the apex), low labeling by JIM5 antibody (for HG epitopes with up to 40 % methylesterification) was observed, possibly indicating that HGs are signals of the final stages of maturation of these cells.

In the mature velamen, HGs occur sometimes in association with lipids and usually with lignins, which represent the development of the secondary cell wall. Lipids and lignins were detected in the cells of the exodermis and were gradually deposited throughout the velamen (obeying a centrifugal direction). Suberin is the main lipid described for the cell walls of the velamen and is hydrophobic and, just like lignins, is responsible for preventing the free flow of water, ions and pathogens by apoplast flow across the exodermis (Schreiber 2010; Joca *et al*. 2017). However, in the velamen, the secondary wall with thick and large highly hydrophobic pores guarantees mechanical resistance and efficient water flow via the apoplasts (Benzing 1986). The large amount of parietal thickenings, representing the secondary walls, ensure a solid surface with several pores (see Fig. 3) which promote a better transport of water throug the velamen, since the transport occurs by mass flow and passively, allowing the root to mobilize water reserves and minerals (Benzing *et al*. 1982).

Main considerations

A still developing green tip was observed in the root apex of the four *Catlleya* species, taking on a white coloration with velamen maturation and filling with air. Close to the RAM, the purple color was derived from the presence of anthocyanins in the vacuole of cortical cells, while the green color (in the subsequent region) was due to the differentiation of chloroplasts. The development of the primary wall led to the deposition of pectins as highly methylesterified HGs, with root maturation undergoing demethylesterification. The deposition of lipids in the velamen cells, and subsequently lignin deposition, marked a transition stage to secondary wall formation, efficiently directing water and nutrients across the simplast of the exodermis. The deposition of lipids and lignins began near the exodermis in the direction of the epivelamen. Before maturation, dead and living cells were intercalated and living cells with a protoplast gave a translucent appearance to the velamen, permitting visualization of the parenchymatic cortex (with chlorophyll). At this stage, wall thickenings were already visible and lignin deposition gave rigidity to the tissue.

Acknowledgements

We thank Universidade Federal de Uberlândia (UFU), the Graduate Program in Plant Biology, the laboratories of Instituto de Biologia (Laboratório de Fisiologia Vegetal and Laboratório de Anatomia, Desenvolvimento Vegetal e Interações). We also thank the Colégio de Aplicação COLUNI of Universidade Federal de Viçosa for kindly supplying the plants. This study was financed in part by the Coordenação de Aperfeiçoamento de Pessoal de Nível Superior - Brasil (CAPES) - Finance Code 001.

References

Albersheim P, Darvill A, Roberts K, Sederoff R, Staehelin A. 2010. Plant cell walls: from chemistry to biology. New York, Garland Science.

Albersheim P, Darvill AG, O'Neill MA, Schols HA, Voragen AGJ. 1996. An hypothesis: the same six polysaccharides are components of the primary cell walls of all higher plants. In: Visser J, Voragen AGJ. (eds.) Pectins and Pectinases. Progress in Biotechnology. Amsterdam, Elsevier. p. 47-55.

Amar AB, Cobanov P, Ghorbel A, Mliki A, Reustle GM. 2010. Involvement of arabinogalactan proteins in the control of cell proliferation of *Cucurbita pepo* suspension cultures. Biologia Plantarum 54: 321-324.

Benzing DH, Friedman WE, Peterson G, Renfrow A. 1982. Shootlessness, velamentous roots and the preeminence of Orchidaceae in the epiphytic biotype. American Journal of Botany 70: 121-133.

Benzing DH. 1986. The vegetative basis of vascular epiphytism. Selbyana 9: 23-43.

Blake AW, McCartney L, Flint JE. 2006. Understanding the biological rationale for the diversity of cellulose-directed carbohydrate-binding modules in prokaryotic enzymes**.** Journal of Biological Chemistry 281: 29321-29329.

Bukatsch F. 1972. Bemerkungen zur doppelfärbung: astrablau-safranin. Mikrokosmos 61: 255.

Burton RA, Gidley MJ, Geoffrey BF. 2010. Heterogeneity in the chemistry, structure and function of plant cell walls. Nature Chemical Biology 10: 724-732.

Campbell MM, Sederoff RR. 1996. Variations in lignin content and composition. Mechanisms of control and implications for the genetic improvement of plants. Plant Physiology 110: 3-13.

Canteri MHG, Renardb CMGC, Bourvellecb CL, Bureau S. 2019. ATR-FTIR spectroscopy to determine cell wall composition: application on a large diversity of fruits and vegetables. Carbohydrate Polymers 212: 186-196.

Chomicki G, Bidel LPR, Jay-Allemand C. 2014. Exodermis structure controls fungal invasion in the leafless epiphytic orchid *Dendrophylax lindenii* (Lindl.) Benth. ex Rolfe. Flora 209: 88-94.

Chomicki G, Bidel LPR, Ming F, *et al*. 2015. The velamen protects photosynthetic orchid roots against UV-B damage, and a large dated phylogeny implies multiple gains and losses of this function during the Cenozoic. New Phytologist 205: 1330-1341.

Cosgrove DJ, Jarvis MC. 2012. Comparative structure and biomechanics of plant primary and secondary cell walls. Frontiers in Plant Science 3: 204. doi: 10.3389/fpls.2012.00204

Cosgrove DJ. 2005 Growth of the plant cell wall. Nature Reviews Molecular Cell Biology 6: 850-861.
Engard CJ. 1944. Morphological identity of the velamen and exodermis in orchids. Botanical Gazette 105: 457-462.
Enstone DE, Peterson CA. 2005. Suberin lamella development in maize seedling roots grown in aerated and stagnant conditions. Plant, Cell & Environment 28: 444-455.
Fahey LM, Nieuwoudt MK, Harris PJ. 2017. Predicting the cell-wall compositions of *Pinus radiata* (radiata pine) wood using ATR and transmission FTIR spectroscopies. Cellulose 24: 5275-5293.
Franke R, Schreiber L. 2007. Suberin - a biopolyester forming apoplastic plant interfaces. Current Opinion in Plant Biology 10: 252-259.
Gierlinger N, Keplinger T, Harrington M, Schwanninger M. 2013. Raman Imaging of Lignocellulosic Feedstock. In: Ven T, Kadla J. (eds.) Cellulose-biomass conversion. Rijeka, Croatia, Intech Open. p. 159-192.
Heimsch C, James L, Seago JR. 2008. Organization of the root apical meristem in Angiosperms. American Journal of Botany 95: 1-21.
Hervé C, Marcus SE, Knox JP. 2011. Monoclonal antibodies, carbohydrate binding modules, and the detection of polysaccharides in plant cell walls. Methods in Molecular Biology 715: 103-113.
Hose E, Clarkson DT, Steudle E, Schreiber L, Hartung W. 2001. The exodermis: a variable apoplastic barrier. *Journal of Experimental Botany* 52: 2245-2264.
Jarvis MC. 1984. Structure and properties of pectin gels in plant cell walls. Plant, Cell & Environment 7: 153-164.
Joca TAC, Oliveira DC, Zotz G, Cardoso JCF, Moreira ASFP. 2020. Chemical composition of the cell walls in velamentous roots of epiphytic Orchidaceae. Protoplasma 257: 103-118.
Joca TAC, Oliveira DC, Zotz G, Winkler U, Moreira ASFP. 2017. The velamen of epiphytic orchids: variation in structure and correlations with nutrient absorption. Flora 230: 66-74.
Johansen DA. 1940. Plant Microtechnique. New York, McGraw Hill Book Co.
Kang X, Kirui A, Widanage MCD, Mentink-Vigier F, Cosgrove DJ, Wang T. 2019. Lignin polysaccharide interactions in plant secondary cell walls revealed by solid-state NMR. Nature Communications 10: 347. doi: 10.1038/s41467-018-08252-0
Karnovsky MJ. 1965. A formaldehyde-glutaraldehyde fixative of high osmolarity for use in electron microscopy. Journal of Cell Biology 27: 137A-138B.
Kedrovski HR, Sajo MG. 2019. What are tilosomes? An update and new perspectives. Acta Botanica Brasilica 33: 106-115.
Kraus JE, Arduin M. 1997. Manual básico de métodos em morfologia vegetal. Rio de Janeiro, Universidade Federal Rural do Rio de Janeiro, Editora Universidade Rural.
Kraus JE, Louro RP, Estelita MEM, Arduin M, Braga MR. 2012. A célula vegetal. In: Appezato-da-Glória B, Carmello-Guerreiro SM. (eds.) Anatomia vegetal. Viçosa, Universidade Federal de Viçosa. p. 32-36.
Krauss BH. 1948. Anatomy of the vegetative organs of the pineapple *Ananas comosus* (L) Merr. I. Introduction, organography, the stem, and the lateral branch or axillary buds. Botanical Gazette 110: 159-217.
Le Gall H, Philippe F, Domon JM, Gillet F, Pelloux J, Rayon C. 2015. Cell wall metabolism in response to abiotic stress. Plants 4: 112-166.
Leroux O, Eder M, Saxe F, *et al*. 2018. Comparative *in situ* analysis reveals the dynamic nature of sclerenchyma cell walls of the fern *Asplenium rutifolium*. Annals of Botany 121: 345-358.
Liu Q, Talbot M, Llevellyn DJ. 2013. Pectin methylesterase and pectin remodeling differ in fiber walls of two *Gossypium* species with very diffentfibre properties. PLOS ONE 8: e65131. doi: 10.1371/journal.pone.0065131
Lorenzo G, Ferrari S, Giovannoni M, Mattei B, Cervone F. 2019. Cell wall traits that influence plant development, immunity, and bioconversion. The Plant Journal 97: 134-147.
Ma F, Peterson CA. 2003. Current insights into the development, structure and chemistry of the endodermis and exodermis of roots. Canadian Journal of Botany 81: 405-421.
Macedo AM. 2013. Efeito da luminosidade em *Dendrobium*. Revista Uningá Review14: 85-98.
Monties B. 1989. Lignins. In: Harborne JB. (ed.) Methods in plant biochemistry. Vol. I. Plant Phenolics. London, Academic Press. p. 113-157.
Moreira ASFP, Filho JPL, Isaias RMS. 2013. Structural adaptations of two sympatric epiphytic orchids (Orchidaceae) to a cloudy forest environment in rocky outcrops of Southeast Brazil. Revista de Biología Tropical 61: 1053-1065.
Moreira ASFP, Isaias RMS. 2008. Comparative anatomy of the absorption roots of terrestrial and epiphytic orchids. Brazilian Archives of Biology and Technology 51: 83-93.
Newman RH. 2004. Carbon-13 NMR evidence for cocrystallization of cellulose as a mechanism for hornification os bleached kraft pulp. Cellulose 11: 45-52.
North GB, Nobel PS. 1994. Changes in root hydraulic conductivity for two tropical epiphytic cacti as soil moisture varies. American Journal of Botany 81: 46-53.
O'Brien TP, Feder N, McCully ME. 1965. Polychromatic staining of plant cell walls by toluidine blue O. Protoplasma 59: 368-373.
Porembski S, Barthlott W. 1988. Velamen radicum micromorphology and classification of Orchidaceae. Nordic Journal of Botany 8: 117-137.
Pridgeon AM, Stern WL, Benzing HD. 1983. Tilosomes in roots of Orchidaceae: morphology and systematic occurrence. American Journal of Botany 70: 1365-1377.
Pridgeon AM. 1987. The velamen and exodermis of orchid roots. In: Arditti J. (ed.) Orchid biology: reviews and perspectives IV. Ithaca, Cornell University Press. p. 139-192.
Proença SL, Sajo MG. 2008. Rhizome and root anatomy of 14 species of Bromeliaceae. Rodriguésia 59: 113-128.
Ralet MC, Crèpeau MJ, Lefèbvre J, Mouille G, Hofte H, Thibault JF. 2008. Reduced number of homogalacturonan domains in pectins of an *Anabidopsis* mutant enhances the flexibility of the polymer. Biomacromolecules 9: 1454-1469.
Ridley B, O'neil MA, Mohnen D. 2001. Pectins: structure, biosynthesis, and oligogalacturonide-related signaling. Phytochemistry 57: 929-967.
Sanford WW, Adanlawo FLS. 1973. Velamen and exodermis characters of West African epiphytic orchids in relation to taxonomic grouping and habitat tolerance. Botanical Journal of the Linnean Society 66: 307-321.
Sass JE. 1951. Botanical microtechnique. 2nd. edn. Ames, Iowa State College Press.
Schreiber L. 2010. Transport barriers made of cutin, suberin and associated waxes. Trends in Plant Science 15: 546-553.
Silva CI, Milaneze-Gutierre MA. 2004. Caracterização morfo-anatômica dos órgãos vegetativos de *Cattleya walkeriana* Gardner (Orchidaceae). Acta Scientiarum 26: 91-100.
Willats WGT, Limberg G, Buchholt HC, *et al*. 2000. Analysis of pectic epitopes recognized by hybridoma and phage display monoclonal antibodies using defined oligosaccharides, polysaccharides, and enzymatic degradation. Carbohydrate Research 327: 309-320.
Willats WGT, McCartney L, Mackie W, Knox JP. 2001. Pectin: cell biology and prospects for functional analysis. Plant Molecular Biology 47: 9-27.
Wolf S, Mouille G, Polloux J. 2009. Homogalacturonan methyl-esterification and plant development. Molecular Plant 2: 851-860.
Zeier J, Schreiber L. 1997. Chemical composition of hypodermal and endodermal cell walls and xylem vessels isolated from *Clivia miniata* (identification of the biopolymers lignin and suberin). Plant Physiology 113: 1223-1231.
Zimmermann HM, Hartmann K, Schreiber L, Steudle E. 2000. Chemical composition of apoplastic transport barriers in relation to radial hydraulic conductivity of corn roots (*Zea mays* L.). Planta 210: 302-311.
Zotz G, Winkler U. 2013. Aerial roots of epiphytic orchids: the velamen radicum and its role in water and nutrient uptake. Oecologia 171: 733-741.